Available online at www.sciencedirect.com
SCIENCE DIRECT®
Biomaterials 25 (2004) 1077–1086
Biomaterials
www.elsevier.com/locate/biomaterials

Influence of freezing rate on pore structure in freeze-dried collagen-GAG scaffolds

Fergal J. O'Brien[a], Brendan A. Harley[b], Ioannis V. Yannas[b], Lorna Gibson[a,*]

[a] *Materials Science and Engineering, MIT, 8-135 77 Mass. Ave, Cambridge, MA 02139, USA*
[b] *Mechanical Engineering, MIT, Cambridge, MA 02139, USA*

Received 26 June 2003; accepted 29 July 2003

Abstract

The cellular structure of collagen-glycosaminoglycan (CG) scaffolds used in tissue engineering must be designed to meet a number of constraints with respect to biocompatibility, degradability, pore size, pore structure, and specific surface area. The conventional freeze-drying process for fabricating CG scaffolds creates variable cooling rates throughout the scaffold during freezing, producing a heterogeneous matrix pore structure with a large variation in average pore diameter at different locations throughout the scaffold. In this study, the scaffold synthesis process was modified to produce more homogeneous freezing by controlling of the rate of freezing during fabrication and obtaining more uniform contact between the pan containing the CG suspension and the freezing shelf through the use of smaller, less warped pans. The modified fabrication technique has allowed production of CG scaffolds with a more homogeneous structure characterized by less variation in mean pore size throughout the scaffold (mean: 95.9 μm, CV: 0.128) compared to the original scaffold (mean: 132.4 μm, CV: 0.185). The pores produced using the new technique appear to be more equiaxed, compared with those in scaffolds produced using the original technique.

Keywords: Collagen; Scaffold; Porosity; Microstructure; Cell adhesion

1. Introduction

Porous scaffolds have been used extensively in tissue engineering to provide a three-dimensional structure for both in vitro studies of cell-scaffold interactions and tissue synthesis as well as in vivo studies of induced tissue and organ regeneration. Regardless of the application, the scaffold material, as well as the three-dimensional structure of the scaffold, have a significant effect on cellular activity. For a biologically active scaffold to promote cell adhesion and growth, it must satisfy a number of constraints. It must be biocompatible and degrade in the body at a rate that allows the scaffold to remain insoluble just for the duration of the critical cellular processes; the products of degradation must also be biocompatible. The chemical composition must incorporate ligands appropriate for the binding of cells specific to each application. The average pore diameter must be large enough for cells to migrate through the pores and small enough to retain a critical total surface area for appropriate cell binding. To allow for transport of cells and metabolites the scaffold must have a high specific surface and large pore volume fraction (generally greater than 90%) as well as an interconnected pore network [1]. Scaffold pore size, pore shape, and pore volume fraction are especially critical as they define the total surface area and special distribution of ligands presented to cells.

Scaffold pore size has been shown to influence cellular activity. The optimal scaffold pore size that allows maximal entry of cells [2] as well as cell adhesion and matrix deposition has been shown to vary with different cell types [3,4]. Scaffold pore size has been observed to influence adhesion, growth, and phenotype of a wide variety of cell types, notably endothelial cells, vascular smooth muscle cells, fibroblasts, osteoblasts, rat marrow cells, chondrocytes, preadipocytes, and adipocytes [5–12]. Scaffold heterogeneity has been shown to lead to variable cell adhesion and to affect the ability of the cell to produce a uniform distribution of extracellular

*Corresponding author. Tel.: +1-617-253-7107; fax: +1-617-258-6275.
E-mail address: ljgibson@mit.edu (L. Gibson).

0142-9612/$ - see front matter © 2003 Elsevier Ltd. All rights reserved.
doi:10.1016/S0142-9612(03)00630-6

matrix proteins [5]. There is also evidence that tissue synthesized in a scaffold with non-uniform pore architecture shows inferior biomechanical properties compared to tissue synthesized in a scaffold with a more uniform pore structure [13]. In scaffolds with equiaxed pores, cells aggregate into spherical structures, while in scaffolds with a more elongated pore shape, cells align with the pore axis [14]. With scaffold pore structure so significantly affecting cellular activity, it is important to be able to manufacture scaffolds with a well-defined pore structure.

This study utilizes a porous, type I collagen-glycosaminoglycan (CG) scaffold that has been successfully used to regenerate skin in burn patients, induce regeneration of the conjunctiva, and to enhance peripheral nerve regeneration across long (>25 mm) gaps [1,15–17]. CG scaffolds have also been used for a wide variety of in vitro studies of cellular migration, contraction, and tissue growth [1,8,14,18–20]. Porous, CG scaffolds have been primarily manufactured using a freeze-drying, or lyophilization, technique [1]. Using this technique, a suspension of collagen and glycosaminoclycans is solidified (frozen); the CG co-precipitate is localized between the growing ice crystals, forming a continuous, interpenetrating network of ice and the coprecipitate [19]. Sublimation of the ice crystals leads to formation of a highly porous sponge. The final pore structure depends on the underlying freezing processes during fabrication. The rapid, uncontrolled quench freezing process typically used in fabricating porous scaffolds via freeze-drying results in space- and time-variable heat transfer through the suspension, leading to non-uniform nucleation and growth of ice crystals and, ultimately, scaffold heterogeneity. In localized regions of poor contact between the pan in which the suspension is frozen and the freeze-dryer shelf, there is a lower rate of ice-crystal nucleation than in neighboring regions, giving increased variation in pore size; due to poor heat conduction and the increased temperature of the suspension at these points, these areas have been termed 'hot spots'. In previous studies using CG scaffolds [18], areas which appeared, by visual inspection, to be heterogeneous were avoided in specimen selection. Selecting samples to avoid 'hot spots' introduces a subjective aspect to using CG scaffolds for tissue engineering, and does not allow for a standardized, fixed sample selection protocol.

The objective of this study was to develop a technique to produce a more uniform scaffold pore structure to present cells with a uniform distribution of ligands. As the conditions of freezing for the CG suspension are most significant in defining pore structure, a new freeze-drying technique that increases homogeneity in the freezing process and reduces local areas of variable nucleation needs to be developed. In this study, the conventional technique of fabricating CG scaffolds was altered in two specific ways in an attempt to increase scaffold homogeneity: the size of the pan used during the freezing process was reduced to increase the pan stiffness and reduce the effects of warping, and the rate of CG suspension freezing was slowed and controlled to reduce the heterogeneous freezing processes observed during conventional CG scaffold fabrication processes.

2. Materials and methods

2.1. Preparation of collagen-glycosaminoglycan copolymer scaffolds

The CG scaffolds were fabricated from a collagen-glycosaminoglycan suspension using a freeze-drying method that has been previously described [15,17]. The CG suspension was produced from microfibrillar, type I collagen isolated from bovine tendon (Integra Life-Sciences, Plainsboro, NJ) and chondroitin-6-sulfate isolated from shark cartilage (Sigma-Aldrich Chemical Co., St. Louis, MO). The collagen, chondroitin-6-sulfate, and 0.05 M acetic acid (pH 3.2) were mixed at 15,000 rpm in an overhead blender (IKA Works, Inc., Wilmington, NC). The temperature of the suspension was maintained at 4°C for the entire mixing process by a cooling system (Brinkman, Westbury, CT) in order to prevent denaturation of the collagen fibers. The final CG suspension contained 0.5 wt% collagen and 0.05 wt% chondroitin-6-sulfate. After mixing, the CG suspension was degassed under vacuum (50 mTorr) for 60 min to remove air bubbles created by the mixing process.

CG scaffolds are traditionally fabricated using a rapid-freeze (quenching) freeze-drying technique where the CG suspension, originally at room temperature, is frozen in a grade 304 stainless steel pan (VirTis, Gardiner, NY) by placing it into a pre-cooled freeze-dryer (VirTis Genesis) at -40°C for 60 min [15]. The temperature of the freeze-dryer shelf is maintained at a constant temperature of -40°C via computer control and the pan is constructed from the same alloy as the freeze-dryer shelves to allow for more uniform heat transfer during freezing. The frozen suspension is then sublimated under a vacuum (<100 mTorr) for 17 h at a temperature of 0°C [15].

2.2. Variation of pan stiffness during freezing

To test the effects of the pan stiffness on the pore structure of CG scaffolds, two series of scaffolds were produced following the standard quench freezing protocol, but in pans with two distinct geometries. The first series of scaffolds were fabricated in the original large stainless steel pans (16.9×25.3 cm), while the second series of scaffolds were fabricated in smaller

(12.4 × 12.4 cm) stainless steel pans. Both the pans were made of the same 18 gauge 304 stainless steel; geometrical differences resulted in a 2.78-fold reduction in pan area and an approximately 6-fold increase in pan stiffness for the smaller pan. The relative warping of the pans was determined by mapping the surface topology of the bottom of each pan using a dial indicator (Starrett, Inc., Athol, MA). Two distinct sample selection protocols were utilized to select 5 pairs of samples from each scaffold sheet for pore size analysis. Samples were either selected from five fixed locations within the scaffold regardless of the apparent scaffold heterogeneity (i.e. areas containing 'hotspots' were not excluded from analysis) in a process termed 'Fixed Selection' (Fig. 1), or samples were selected from five areas of the scaffold deemed by visual inspection to be the most homogeneous (i.e. 'hot spots' were excluded) in a process termed 'Best Pick Selection.' Scaffolds produced in the smaller pans did not exhibit heterogeneities visible to the naked eye; consequently, samples were removed for analysis using only the 'Fixed Selection' technique.

2.3. Varying suspension cooling rate during freezing

The cooling rate of the freeze-dryer shelf was varied in order to test the effects of variable freezing conditions on the final scaffold structure. With the constant cooling rate technique, the CG suspension was placed into the chamber of the freeze-dryer at room temperature (20°C) and the temperature of the chamber and shelf of the freeze-dryer was then reduced (ramped) at a constant rate via computer control to the final freezing temperature (−40°C); the temperature was then held constant at −40°C for 60 min. The ice phase was then sublimated under vacuum (<100 mTorr) at 0°C for a period of 17 h as has previously been described [15]. The term "constant cooling rate" refers to the constant cooling rate of the freeze-dryer shelf and not to the cooling rate of the CG suspension, which will be characterized separately. The CG suspension was frozen at three distinct cooling rates, where the freeze-dryer shelf temperature was ramped from 20°C to the final temperature of −40°C in 65, 90 and 115 min. A fourth scaffold was produced using the quenching technique previously described. Samples were removed for pore analysis from all four types of scaffold using the 'Fixed Selection' protocol previously described. All samples were made using the smaller pans.

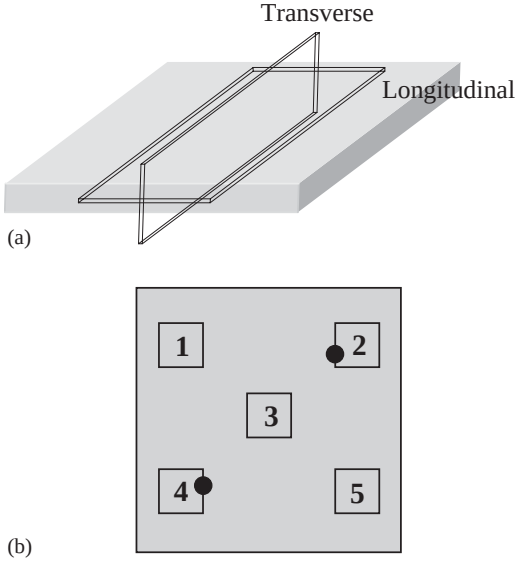

Fig. 1. Orientation of longitudinal and transverse planes used during pore size analysis (Fig. 1a) as well as the locations where samples were removed for analysis via the fixed selection protocol (1–5) and the location (●) of the thermocouples during measurement of the freezing kinetics of the CG suspension (Fig. 1b).

The temperature of the CG suspension was monitored at 1 min intervals until sublimation at two locations in the suspension using a two-channel microprocessor thermocouple (HH22, Omega Engineering, Stamford, CT). Two thermocouple elements (Type K Thermocouple, Omega Engineering, Stamford, CT) were placed approximately 10 cm apart along a diagonal between the opposite corners of the pan (Fig. 1). The average freezing rate of the suspension (in °C/min) for all freezing protocols was computed between the starting temperature and −30°C. The lower limit of −30°C was used in this calculation because below that temperature, the temperature of the suspension and the freeze-dryer shelf tended to asymptotically approach the final temperature of freezing, and could not be modeled linearly. The liquid–solid transition time, corresponding to the time where liquid and solid coexist, is a measure of how rapidly the suspension begins to solidify [21]; it was measured as the time that the suspension temperature remained between 0°C and −1°C following the initial supercooling condition required to initiate ice crystal nucleation.

2.4. CG scaffold crosslinking

All CG scaffolds were dehydrothermally crosslinked in order to stiffen the collagen network. Cross-linking was carried out under a vacuum (50 mTorr) in a vacuum oven (Fisher IsoTemp 201, Fisher Scientific, Boston, MA) at a temperature of 105°C for 24 h [15,17]; this process introduces covalent cross-links between the polypeptide chains of the collagen fibers without denaturing the collagen into gelatin [22]. Following cross-linking, the pore characteristics of the scaffolds were analyzed.

2.5. Analysis of pore structure

To determine the average pore size of the scaffolds, pairs of samples were removed from five locations in

each sheet of the CG scaffold. At each of the five locations, samples were obtained to analyze the longitudinal (10×10 mm square section) and transverse (10×5 mm rectangular section) planes (Fig. 1). Each of these samples was cut from the top surface through the entire depth of the scaffold (approximately 3 mm). The sections were embedded in glycolmethacrylate, serially sectioned on a Leica RM2165 microtome (Mannheim, Germany) at a 5 μm thickness, stained using aniline blue and visualized on an optical microscope (Nikon Optiphot, Japan).

Three digital images of each longitudinal section and two images of each of the smaller transverse sections were taken using a CCD color video camera (Optronics Engineering, Inc., Goleta, CA). A total of 125 digitized images (25 images from each of five locations per scaffold) were analyzed from each scaffold sheet using a linear intercept macro written for Scion Image™ image analysis software (Scion Corp., Frederick, MD) [20]. The program constructed a best-fit ellipse representing an average pore cross-section for each image analyzed. To account for the effects of pores that were not sectioned through their maximal cross-section but rather at an arbitrary angle, the ellipse major and minor axes were corrected by multiplying by 1.5 [23]. The mean intercept length was an average of the major and minor axes of this reconstructed best-fit shape. The mean pore diameter of the scaffold at each position within the scaffold was calculated from the average of the mean intercepts in the longitudinal plane and in the adjacent transverse plane [20].

2.6. Environmental scanning electron microscopy

Environmental scanning electron microscopy (ESEM) was used to qualitatively compare the pore structure of the scaffolds produced by the original quenching technique and the constant cooling rate technique. Cylindrical sections, 9 mm in diameter, were removed from the thickness of the scaffold and stored in phosphate buffered saline (PBS, Sigma-Aldrich Chemical Co., St. Louis, MO) prior to observation. The hydrated samples were removed from the PBS and placed directly onto the sample holder attached to the Peltier cooling stage in the ESEM without the need of prior sputter coating.

2.7. Micro computed-tomography

The three-dimensional structure of a scaffold manufactured using the original quenching technique was analyzed using micro computed-tomography (Micro-Photonics, PA), to obtain a separate quantitative measurement of pore size, in order to confirm the scaffold pore analysis by the linear intercept method. Scans were performed on a Skyscan 1072 Micro-CT system (Aartselaar, Belgium) with 100 keV X-ray source and a 12 bit cooled CCD camera. Cross-sections were generated using a full cone beam Feldkamp reconstruction algorithm. Morphological calculations were carried out on the reconstructed sections using the standard Skyscan software package to calculate the mean pore size of the scaffold.

2.8. Statistical analysis

Paired *t*-tests were performed to compare individual sets of data to determine statistical significance. One-way analysis of variance (ANOVA) and pair-wise multiple comparison procedures (Tukey Tests) were used to compare data groups. Error is reported in the text and figures as the standard deviation or as the coefficient of variance (CV = standard deviation/mean) in order to compare the relative variation in pore size between different scaffolds. A probability value of 95% ($p < 0.05$) was used to determine significance.

3. Results

3.1. Influence of pan size on pore size

Visual inspection revealed that the CG scaffolds produced in the smaller stainless steel pan were more homogeneous than those prepared in the larger stainless steel pan, with no apparent 'hot spots' due to variable nucleation of ice crystals. Fig. 2 shows the results of the pore size analysis of scaffolds produced using the large and small stainless steel pans. One-factor ANOVA indicated a significant effect of pan size and sample selection method on the pore structure ($p < 0.05$). The mean pore size of scaffolds produced using the smaller pan (Fixed Selection) was found to be significantly

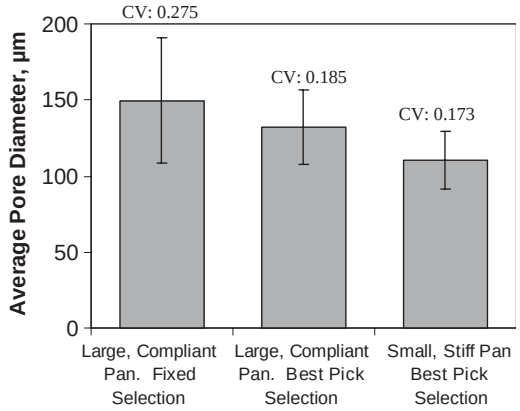

Fig. 2. The effect of pan size and stiffness on the mean pore size and on scaffold homogeneity. No 'hotspots' due to variable nucleation were found in scaffolds manufactured in the smaller, less warped stainless steel pan, and those scaffolds showed a smaller mean pore size with reduced scaffold heterogeneity.

smaller ($p<0.05$) than that of scaffolds produced in the larger, more compliant stainless steel pan (both Fixed Selection and Best Pick). The coefficient of variance (CV) of the pore size of scaffolds produced in the smaller pans (Fixed Selection) was found to be significantly smaller ($p<0.05$) than that of scaffolds produced in the large pan (Fixed Selection). However, when inhomogeneities were avoiding in selecting samples from the large pan (Best Pick Selection), the CV of the mean pore size of scaffolds was not significantly different than that for scaffolds produced in the smaller pan (Fixed Selection) ($p = 0.09$). Nevertheless, the use of the small pans removes a subjective element from the selection of samples from the scaffolds. There was an overall improvement of scaffold homogeneity by using the smaller pans. Analysis of the surface topology of the pans provides an explanation for this.

The average deflection at the center of the pan for the larger, more compliant pans (254 μm) was considerably larger than for the smaller, stiffer pans (80 μm). The relative pan warping of the larger and smaller pans was determined by comparing the average standard deviation of the deflection of the pan along the rows and columns of the grid used to measure the relative pan heights across the bottom. The average standard deviation of the deflection of the pan for the larger pans (144.6 ± 71.4 μm) was significantly larger ($p = 0.002$) than that of the smaller pans (45.7 ± 18.0 μm). These results suggest that the smaller pans are significantly less warped and show a smaller overall deflection compared to the larger pans. The increased stiffness of the smaller pan is expected to reduce warping from repeated freeze–thaw cycles.

3.2. Control of the rate of freezing of the CG suspension

Fig. 3 shows the average temperature of the CG suspension during freezing for the quenching and the constant cooling rate techniques. A larger absolute difference in slurry temperature was observed between measurement locations during the freezing process (larger error bars) for the quenching technique as compared to the constant cooling rate technique. One-factor ANOVA indicated a significant effect of freezing technique on the temperature variation throughout the pan ($p<0.0001$). The constant cooling rate technique with a freezing time of 65 min displayed significantly improved freezing homogeneity compared to the quenching technique ($p<0.0001$) and the constant cooling rate technique with a freezing time of 105 min ($p<0.0001$), but not compared to the constant cooling rate technique with a freezing time of 90 min ($p = 0.52$). Table 1 shows the results of measurements of the average freezing rate of the slurry and the time required for the liquid–solid transition of the CG suspension at the point of freezing. The quenching technique showed the most rapid freezing rate (4.1°C/min) with the shortest duration at the liquid–solid transition (2 min) while the constant cooling rate protocols had significantly slower rates of freezing (0.9°C, 0.7°C, 0.6°C/min) and longer liquid–solid transition times (10.5, 11, 14.5 min) for freezing times of 65, 90 and 105 min, respectively.

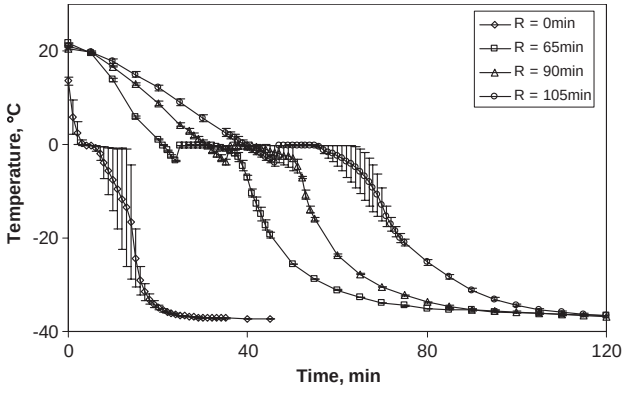

Fig. 3. Average temperature of the CG suspension during freezing recorded at two distinct positions within the pan (error bar: half the difference between two temperature readings) for the four freezing curves (R = length in min of the constant cooling period during the freezing process).

3.3. Influence of rate of freezing on pore size

The cellular structure of scaffolds produced using the constant cooling rate technique (0.9°C/min) appears significantly more homogeneous throughout the entire scaffold than the scaffold structure produced using the original quenching technique (Fig. 4). Although locally, pores often tended to be aligned in a particular direction, no consistency of pore orientation was found between the five separate sampling locations in both the quenching and the constant cooling rate techniques. When the scaffolds are compared, it is apparent that using the new constant cooling rate technique, the pores are more uniform in size, have a consistent pore structure, and show no obvious variation in mean pore size, pore structure, or alignment throughout the scaffold, differing significantly from scaffolds fabricated using the quenching protocol. Similar results were found for analysis of both the transverse and longitudinal sections.

Table 1
Freezing rate of CG suspension and the time required for the liquid–solid transition during freezing

Freezing time	Average suspension freezing rate (°C/min)	Liquid–solid transition time (min)
Quenching	4.1	2
65 min	0.9	10.5
90 min	0.7	11
105 min	0.6	14.5

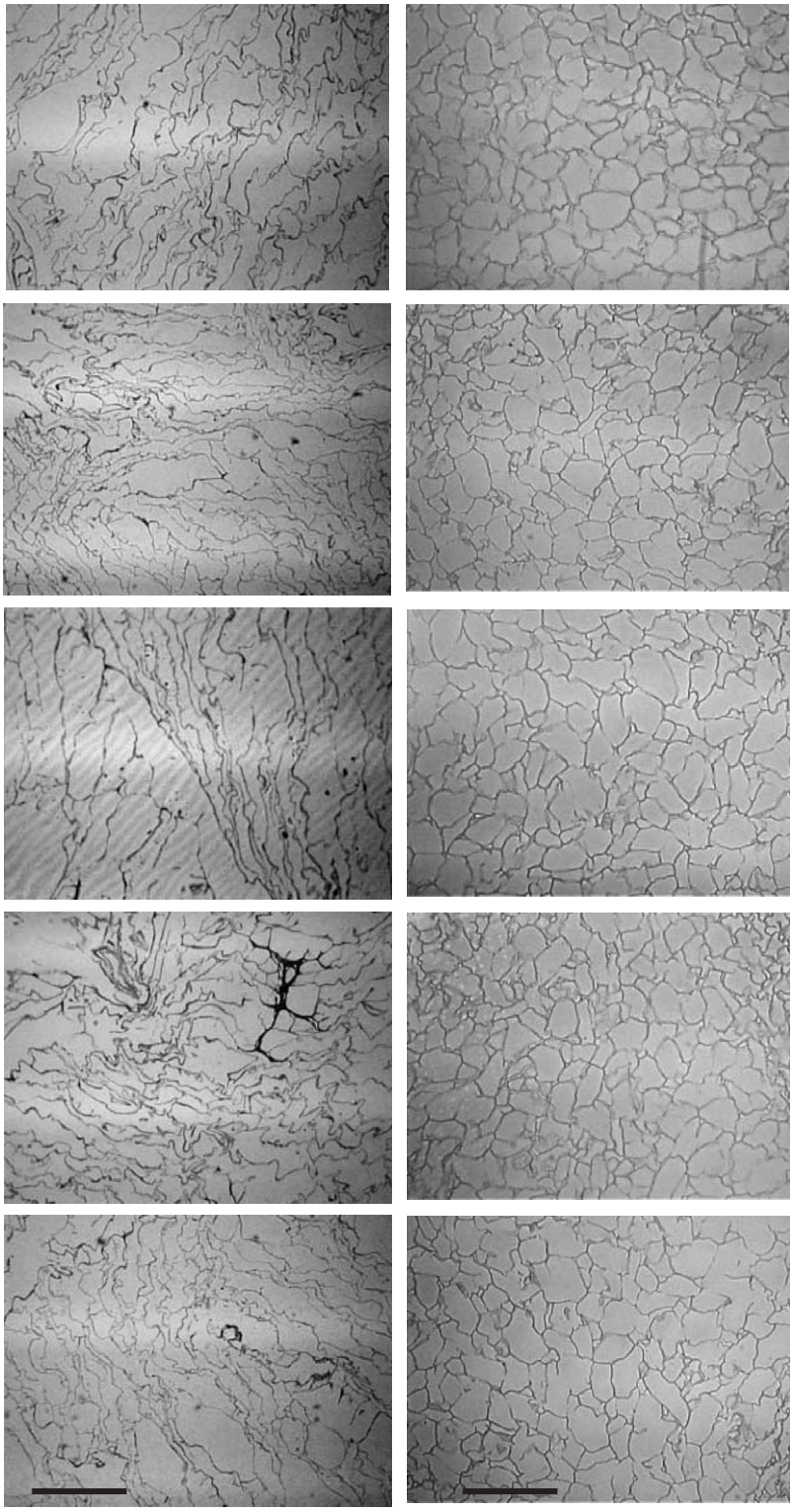

(a) (b)

Fig. 4. A series of longitudinal images taken via the fixed selection protocol from a single sheet of scaffold produced using the quenching (Fig. 4a) and the constant cooling rate technique that displayed the greatest freezing rate homogeneity (0.9°C/min) (Fig. 4b). The constant cooling rate technique produced pores with a more uniform size and structure at each sample point (locally), and also a more homogeneous nature throughout the scaffold (globally). Scale bar = 300 μm.

ESEM micrographs (Fig. 5) indicate that the pore structure of the scaffold produced using the quenching technique (4.1°C/min) is characterized by roughly parallel planes of collagen that are separated by thin collagen struts while the pore structure of the scaffold produced using the constant cooling rate technique (0.9°C/min) is characterized by more randomly oriented solid collagen struts and membranes, corresponding to a more equiaxed pore structure.

When examined with the naked eye, all scaffolds produced using the constant cooling rate techniques (0.9°C, 0.7°C, and 0.6°C/min) appear to be homogeneous in nature throughout the entire scaffold with no evident 'hot spots.' The histomorphometric analysis of scaffolds produced using the quenching and the constant cooling rate techniques indicate that scaffolds fabricated with the constant cooling rate technique are more uniform than those produced with the quenching technique (Fig. 6). A significantly higher coefficient of variance (0.173) was found for the scaffold produced using the original quenching technique ($p<0.05$) compared to the three scaffolds formed using the constant cooling rate technique. The scaffold produced by freezing at a rate of 0.9°C/min was found to produce the most uniform scaffold, with a smaller coefficient of variance (0.128) compared to those observed for the other two rates of freezing (values of 0.146 and 0.151 for freezing rates of 0.7°C and 0.6°C/min, respectively) ($p<0.05$). In addition, scaffolds produced at a freezing rate of 0.9°C/min were also found to have a significantly smaller mean pore size ($p<0.05$) compared to the more rapid (4.1°C/min) and slower rates of freezing (0.7°C and 0.6°C/min).

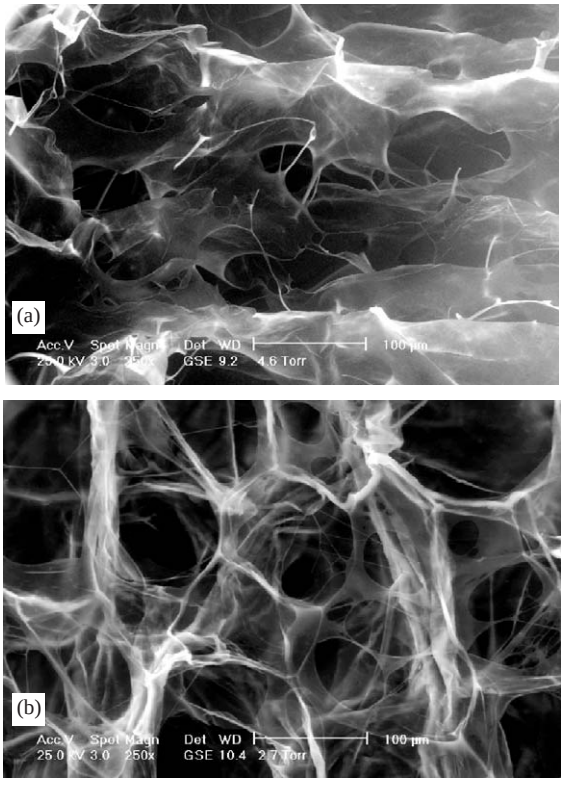

Fig. 5. ESEM micrographs of CG scaffolds produced using the quenching technique in the large pans (Fig. 5a) and the constant cooling rate technique (0.9°C/min) in the small pans (Fig. 5b).

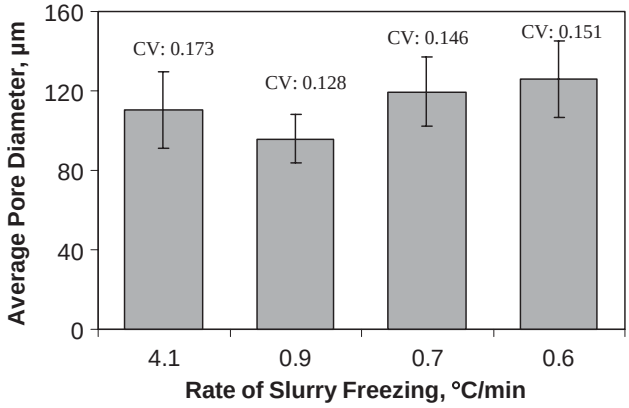

Fig. 6. Average pore size for scaffolds fabricated with the quenching (4.1°C/min) and the constant cooling rate technique (0.9°C, 0.7°C, 0.6°C/min) in the small stainless steel pans.

This study demonstrated that a freezing rate of 0.9°C/min, corresponding to a more controlled freezing process than the original quenching protocol, produced a scaffold with a more homogeneous structure than the other techniques studied. Further analysis was conducted to determine whether uniform scaffolds could be produced consistently. Three scaffolds were produced in the smaller stainless steel pans using a freezing rate of 0.9°C/min, with results shown in Fig. 7. No significant difference in mean pore size was found between the scaffolds ($p=0.257$), and a CV of less than 0.167 was found for each sheet. This data indicates that a constant cooling rate of 0.9°C/min consistently produces a more homogeneous scaffold than the standard quenching technique.

3.4. Pore structure and anisotropy

The mean pore size of scaffolds in the longitudinal and transverse planes, at five locations within the scaffold is shown in Fig. 8 for scaffolds made by the quenching (Fig. 8a) and the constant cooling rate technique (0.9°C/min) (Fig. 8b) in the small pans. The quenching technique produces a significant variation in the mean pore size between locations throughout the scaffold ($p<0.001$) and between the longitudinal ($114.9\pm17.7\,\mu m$) and transverse ($102.7\pm18.6\,\mu m$) planes ($p<0.05$). For scaffolds produced by the constant cooling rate technique, no significant difference in mean pore size was found at the five sample points within each sheet ($p=0.177$) or between the longitudinal ($96.8\pm11.1\,\mu m$) and the transverse planes ($94.2\pm13.9\,\mu m$) in the scaffold ($p=0.313$). While scaffolds produced

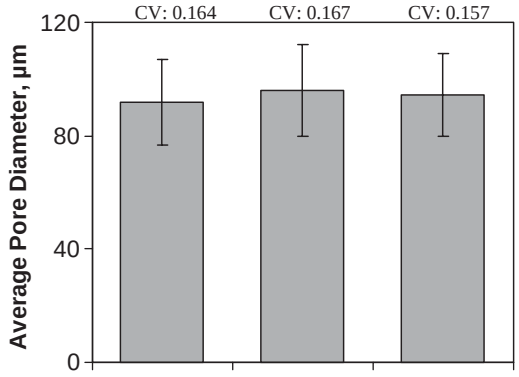

Fig. 7. Sheet-to-sheet variability of the mean pore size of three CG scaffolds produced with an average shelf-freezing rate of 0.9°C/min.

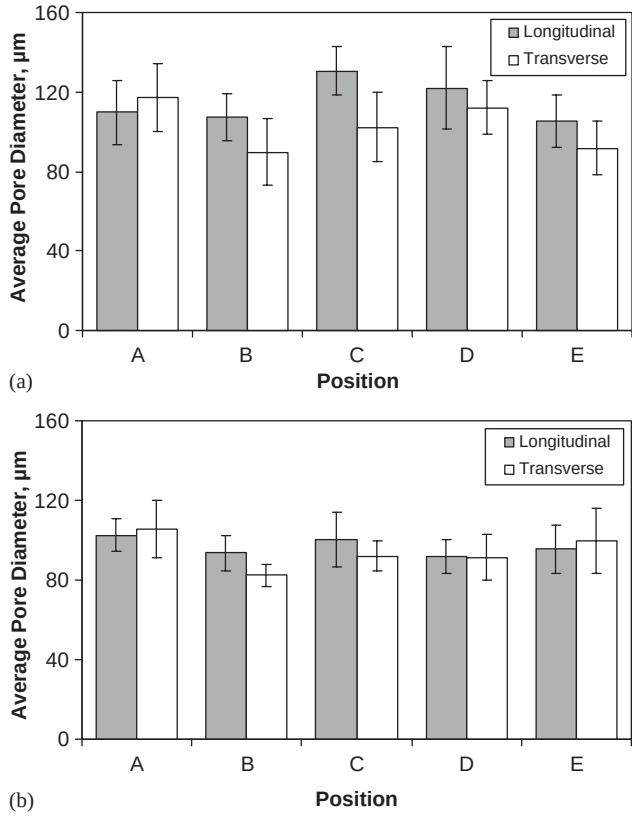

Fig. 8. Analysis of pore structure at five locations throughout the CG scaffold in both the longitudinal and transverse planes of scaffolds produced using quenching (Fig. 8a) and the constant cooling rate technique (0.9°C/min) (Fig. 8b). Scaffolds manufactured through quenching showed an average pore size of $114.9 \pm 17.7\,\mu m$ and $102.7 \pm 18.6\,\mu m$, while scaffolds produced using the constant cooling rate technique had an average pore size of $96.8 \pm 11.1\,\mu m$ and $94.5 \pm 13.9\,\mu m$ in the longitudinal and transverse planes, respectively.

using the quenching technique show a significant spatial variation of mean pore size as well as oriented pores (significantly longer longitudinal than transverse mean intercept), scaffolds produced with the constant cooling rate technique show no significant spatial variation in pore size as well as equiaxed pores.

3.5. Micro CT analysis

A section of a CG scaffold (Best Pick Selection) fabricated using the quenching technique in the large stainless steel pans was analyzed via micro-CT (Skyscan 1072 Micro-CT system). A mean pore size of 130 µm was calculated from analysis of a series of scans. The result of this calculation compares favorably with the mean pore size calculated from the linear intercept method (132.4 µm).

4. Discussion

Collagen-GAG scaffolds manufactured using the original (quenching) freeze-drying technique [15] show a characteristic heterogeneous pore structure with a large variation in average pore diameter at different locations and orientations (in and out of plane) in each sheet of scaffold. Control of the rate of cooling during fabrication and the use of smaller, less warped stainless steel pans significantly improved the structural characteristics of the scaffold: a more homogeneous structure with less variation in mean pore size throughout the scaffold and no difference in pore size between the transverse and longitudinal planes was observed.

The structure of the collagen scaffold is controlled by the final temperature of freezing and the heat transfer processes associated with freezing. Furthermore, the formation of ice crystals within the CG suspension is influenced by both the rate of nucleation of ice crystals and the rate of heat and protein diffusion. The nucleation rate defines the number of ice crystals that form and the rate of heat and protein (collagen-glycosaminoglycan) diffusion away from the point of nucleation defines the size of ice crystals. Both the rate of nucleation and diffusion are mediated by the difference between the temperature of freezing and the actual temperature of the material during the freezing process, termed undercooling [24]. A larger undercooling has been demonstrated to lead to an increased rate of nucleation of ice crystals with a decreased heat and protein diffusion rate away from the point of nucleation [24,25]. Therefore, with larger undercooling, smaller ice crystals are formed, leading to a CG scaffold with a smaller average pore diameter following sublimation [16,26]. Additionally, the direction of heat transfer and the speed of heat transfer influence the shape of ice crystals; the existence of a predominant direction of heat transfer leads to the formation of columnar ice crystals with the major axis aligned in the predominant direction of heat transfer [16,26–28]. Creation of a scaffold with an equiaxed pore structure requires removing predominant direction of heat transfer from the freezing process.

When the quenching fabrication technique was used in conjunction with the larger, more warped, stainless steel pans to produce CG scaffolds, 'hot spots' were created throughout the scaffold due to areas of pan-shelf discontinuity. When these areas were included in the analysis of the pore structure, a significantly larger mean pore size with a significantly larger co-efficient of variance was found (Mean: 149.6 μm, CV: 0.275) than when the areas were avoided (Mean: 132.4 μm, CV: 0.185), validating previous studies where these areas were avoided [19]. In order to avoid formation of such sites, a series of new smaller, less warped pans were introduced. The scaffolds produced using these pans showed no visual evidence of 'hot spots' to the naked eye. While a smaller mean pore size and lower coefficient of variance (CV: 0.173) was observed with the scaffolds produced in the smaller pans using the quenching technique, the improvements were not significantly improved ($p > 0.05$) compared to selection of the "best" areas from scaffolds produced in large pans with the quenching technique.

As a second component of this study, a comparison was made between the quenching process and a series of constant cooling rate freezing protocols. All scaffolds produced for this portion of the study were fabricated in the smaller, stiffer stainless steel pans. Three distinct constant cooling rates were tested by cooling the freeze-dryer from 20°C to −40°C over 65, 90, or 115 min, corresponding to average slurry freezing rates of 0.9°C, 0.7°C, and 0.6°C/min, respectively. The scaffolds produced using the constant cooling rate technique were observed to have a more homogeneous pore structure than those produced using the quenching technique (Fig. 4). This result parallels the finding that the quenching process gives rise to a wide variation in suspension temperature throughout the pan during freezing, while the constant cooling rate process produces virtually identical suspension temperatures throughout the pan during freezing. Scaffolds produced using a constant cooling rate of 0.9°C/min were found to have the most homogeneous structure with the lowest coefficient of variance in pore size (0.128) and the smallest difference in pore size between the longitudinal and transverse planes in the scaffold. This freezing protocol also exhibited the greatest level of temperature uniformity during freezing (Fig. 3). A series of scaffolds were manufactured at this constant cooling rate (0.9°C/min) in order to establish the reproducibility of this protocol. The scaffold pore size was found to be consistent from sheet to sheet, the coefficient of variance was found to be consistently smaller than under previous processing conditions, and no 'hotspots' were found in any of the scaffolds manufactured with a constant cooling rate of 0.9°C/min. These results suggest that the constant cooling rate technique establishes a more uniform temperature distribution throughout the suspension during freezing, resulting in consistent ice crystal nucleation and growth and a more uniform final scaffold structure.

Fig. 6 shows an in-depth comparison of the pore size distribution in two scaffold types: a scaffold fabricated using the quenching technique and a scaffold fabricated using a constant cooling rate of 0.9°C/min. CG scaffolds produced using the constant cooling rate technique (0.9°C/min) showed significantly smaller variation in pore size throughout the scaffold and no variation in mean intercept length between the longitudinal and transverse planes while the scaffold manufactured using the quenching protocol had a considerably larger variation in pore size throughout the scaffold and in the longitudinal and transverse planes. These results suggests that there is reduced variation in pore size throughout the scaffold along with an equiaxed pore structure when the scaffold is manufactured using the constant cooling rate technique (0.9°C/min). ESEM micrographs of the scaffold pore structure (Fig. 5) further support this conclusion; in the scaffold produced using the constant cooling rate technique, the collagen fibers (struts) are randomly arranged around approximately equiaxed pores while in the scaffold produced using the original quenching technique, there are roughly parallel planes of collagen membranes separated by thin collagen struts. Overall, the pores produced using the new technique appear to be more equiaxed unlike the elongated pores in scaffolds produced using the quenching technique. Additionally, while pore orientation in scaffolds fabricated using the quenching technique in large pans (original technique) was observed to be grossly random, pore alignment was observed locally, indicating areas of directional heat transfer. However, the pore structure of the CG scaffolds produced using the constant cooling rate technique was observed to be equiaxed with no local or global alignment of pores, indicating the effects of local heat transfer phenomena were removed from the fabrication process (Figs. 4, 5 and 8).

5. Conclusions

This investigation has shown that uniform CG scaffolds with an equiaxed pore structure can be produced via lyophilization with the use of a constant cooling rate technique rather than a quenching technique to freeze the CG suspension prior to sublimation. The constant cooling technique establishes a more uniform suspension temperature throughout the pan during the freezing process compared to the quenching technique, where the constant cooling rate that produced the most uniform temperature distribution also produced the most uniform scaffold structure. The most uniform scaffolds displayed approximately equiaxed

pores, with no significant pore size variation throughout the scaffold. These results indicate that significantly more uniform porous scaffolds can be manufactured for tissue engineering applications using a constant cooling rate freezing technique.

Acknowledgements

We are grateful for the funding for this study provided by the Cambridge-MIT Institute (FJO, BAH, IVY, LJG) and the Fulbright Program (FJO). We are grateful to Shona Pek of the Cellular Solids Group in MIT for carrying out the ESEM analysis, MicroPhotonics Inc. (Allentown, PA) for carrying out the micro-CT analysis on our samples, Yihvan Vuong for assisting the relative pan warping analysis, and to the Edelmann Laboratory in MIT for use of their facilities during histological preparation of samples.

References

[1] Yannas IV. Tissue and organ regeneration in adults. New York: Springer; 2001.
[2] Chvapil M. Collagen sponge: theory and practice of medical applications. J Biomed Mater Res 1977;11:721.
[3] Tsuruga E, Takita H, Itoh H, Wakisaka Y, Kuboki Y. Pore size of porous hydroxyapatite as the cell-substratum controls BMP-induced osteogenesis. J Biochem 1997;2:317–24.
[4] Doillon CJ, Whyne CF, Brandwein S, Silver FH. Collagen-based wound dressings: control of the pore structure and morphology. J Biomed Mater Res 1986;8:1219–28.
[5] Zeltinger J, Sherwood JK, Graham DA, Mueller R, Griffith LG. Effect of pore size and void fraction on cellular adhesion, proliferation, and matrix deposition. Tissue Eng 2001;7(5):557–72.
[6] Wake MC, Patrick Jr. CW, Mikos AG. Pore morphology effects on the fibrovascular tissue growth in porous polymer substrates. Cell Transplant 1994;3(4):339–43.
[7] Salem AK, Stevens R, Peason RG, Davies MC, Tendler SJ, Roberts CJ, Willams PM, Shakesheff KM. Interactions of 3T3 fibroblasts and endothelial cells with defined porefeatures. J Biomed Mater Res 2002;61(2):212–7.
[8] Nehrer S, Breinan HA, Ramappa A, Young G, Shortkroff S, Louie LK, Sledge CB, Yannas IV, Spector M. Matrix collagen type and pore size influence behavior of seeded canine chondrocytes. Biomaterials 1997;18(11):769–76.
[9] LiVecchi AB, Tombes RM, LaBerge M. In vitro chondrocyte collagen deposition within porous HDPE: substrate microstructure and wettability effects. J Biomed Mater Res 1994;28(8):839–50.
[10] Kuberka M, von HD, Schoof H, Heschel I, Rau G. Magnification of the pore size in biodegradable collagen sponges. Int J Artif Organs 2002;1:67–73.
[11] Claase MB, Grijpma DW, Mendes SC, De Bruijn JD, Feijen J. Porous PEOT/PBT scaffolds for bone tissue engineering: preparation, characterization, and in vitro bone marrow cell culturing. J Biomed Mater Res 2003;64A:291–300.
[12] Borden M, El-Amin SF, Attawia M, Laurencin CT. Structural and human cellular assessment of a novel microsphere-based tissue engineered scaffold for bone repair. Biomaterials 2003; 24:597–609.
[13] Hollister SJ, Maddox RD, Taboas JM. Optimal design and fabrication of scaffolds to mimic tissue properties and satisfy biological constraints. Biomaterials 2002;23(20):4095–103.
[14] Zmora S, Glicklis R, Cohen S. Tailoring the pore architecture in 3-D alginate scaffolds by controlling the freezing regime during fabrication. Biomaterials 2002;23(20):4087–94.
[15] Yannas IV, Lee E, Orgill DP, Skrabut EM, Murphy GF. Synthesis and characterization of a model extracellular matrix that induces partial regeneration of adult mammalian skin. Proc Natl Acad Sci USA 1989;86(3):933–7.
[16] Chang AS, Yannas IV. Peripheral nerve regeneration. In: Smith B, Adelman G, editors. Encyclopedia of neuroscience. Boston: Birkhauser; 1992. p. 125–6.
[17] Chamberlain LJ, Yannas IV, Hsu HP, Strichartz G, Spector M. Collagen-GAG substrate enhances the quality of nerve regeneration through collagen tubes up to level of autograft. Exp Neurol 1998;154(2):315–29.
[18] Freyman TM, Yannas IV, Yokoo R, Gibson LJ. Fibroblast contraction of a collagen-GAG matrix. Biomaterials 2001;22(21): 2883–91.
[19] Freyman TM, Yannas IV, Gibson LJ. Cellular materials as porous scaffolds for tissue engineering. Prog Mater Sci 2001;46: 273–82.
[20] Freyman TM. Development of an In Vitro Model of Contraction by Fibroblasts. Ph.D. Thesis, Massachusetts Institute of Technology, 2001.
[21] Michel B. Ice Mechanics, Quebec: Les Presses De L'Universite Laval, 1978.
[22] Yannas IV. Collagen, gelatin in the solid state. Rev Macromol Chem 1972;C7:49–104.
[23] Gibson LJ, Ashby MF. Cellular solids: structure and properties. Cambridge: Cambridge University Press; 1997.
[24] Kurz W, Fisher DJ. Fundamentals of solidification. Switzerland: Transtech Publications; 1989.
[25] Hobbs PV. Ice physics. Oxford: Clarendon Press; 1974.
[26] Chang AS, Yannas IV, Perutz S, Loree H, Sethi RR, Krarup C, Norregaard, Zervas NT, Silver J. Electrophysiological study of recovery of peripheral nerves regenerated by a collagen-glycosaminoglycan copolymer matrix. In: Gebelin CG, Dunn RL, editors. Progress in biomedical polymers. New York: Plenum Press; 1990. p. 107–19.
[27] Schoof H, Apel J, Heschel I, Rau G. Control of pore structure and size in freeze-dried collagen sponges. J Biomed Mater Res 2001;58(4):352–7.
[28] Loree HM, Yannas IV, Mikic B, Chang AS, Perutz SM, Norregaard TV, Krarup C. A freeze-drying process for fabrication of polymeric bridges for peripheral nerve regeneration. Proceedings of the 15th Annual Northeast Bioengineering Conference, 1989, p. 53–4.